Published in final edited form as:
J Nat Prod. 2007 October ; 70(10): 1551–1557. doi:10.1021/np070088v.

Induction of Apoptosis by Diterpenes from the Soft Coral *Xenia elongata*

Eric H. Andrianasolo[†], **Liti Haramaty**[†], **Kurt Degenhardt**[‡], **Robin Mathew**[§,⊥], **Eileen White**[‡,§,⊥], **Richard Lutz**[†], and **Paul Falkowski**[*,†]

[†]Center for Marine Biotechnology, Institute of Marine and Coastal Sciences, Rutgers, The State University of New Jersey, Piscataway, New Jersey 08901-8521

[‡]Center for Advanced Biotechnology and Medicine, Department of Molecular Biology and Biochemistry, Rutgers, The State University of New Jersey, 679, Hoes Lane, Piscataway, New Jersey 08854

[§]University of Medicine and Dentistry of New Jersey, Robert Wood Johnson Medical School, 675 Hoes Lane, Piscataway, New Jersey 08854

[⊥]The Cancer Institute of New Jersey, 195 Little Albany Street, New Brunswick, New Jersey 08903

Abstract

Four new diterpenes (**1**–**4**) were isolated from the soft coral *Xenia elongata* using a novel cell-based screen for apoptosis-inducing, potential anticancer compounds. The molecular structures of the diterpenes were determined using a combination of NMR and mass spectrometry. The bioactivities were confirmed using a specific apoptosis induction assay based on genetically engineered mammalian lines with differential, defined capacities for apoptosis. The diterpenes induce apoptosis in micromolar concentrations. This is the first report of apoptosis induction by marine diterpenes in xenicane skeletons.

Screening organic extracts from marine algae and cyanobacteria for mechanism-based anticancer agents has been quite productive and has led to the discovery of new chemotypes showing antiproliferative properties.[1,2] For the treatment of cancer, cytotoxic chemotherapeutics currently in use rely on the ability to selectively target proliferating cells, which are enriched in tumors. Tumor cells progressively evolve genetic mutations that enable not only cell proliferation but also resistance to programmed cell death, or apoptosis, a cell suicide pathway that is the cellular response to oncogene activation or irreparable cellular damage.[3-6] Effective cancer therapeutic strategies often rely on preferential and efficient induction of apoptosis in tumor cells. Progressive exposure to such molecules commonly leads to selection of resistant cells that are therapeutically associated with both tumor progression and resistance to chemotherapy.[3-6] While many conventional cytotoxic chemotherapeutics trigger apoptosis indirectly by inflicting cellular damage, recent efforts have been directed to developing agents that specifically target or activate the apoptotic pathway irreversibly.[7]

In our ongoing effort to discover and develop new marine natural product biomedicinals, we have screened extracts from several marine organisms and have found that those isolated from a soft coral, *Xenia elongata*, possessed a remarkable ability to specifically induce apoptosis in precancerous, immortal mammalian epithelial cells. Subsequently, extracts were subjected to

*To whom correspondence should be addressed. Tel: (732) 932-6555, ext. 370. Fax: (732) 932-4083. falko@imcs.marine.rutgers.edu..

bioassay-guided purification that resulted in the isolation of four novel diterpenes (**1**–**4**), which we demonstrate are capable of inducing apoptosis in genetically engineered mouse cell lines. To our knowledge, this is the first report of apoptosis induction by marine diterpenes in the xenicane skeletons.

Results and Discussion

Live colonies of *X. elongata* were grown for over three years in the coral laboratory at the Marine Biotechnology Center, Institute of Marine and Coastal Sciences, Rutgers University.

For extraction, 100 to 200 g of the colonies was isolated and frozen. A methanol (or dichloromethane)-soluble fraction was extracted from frozen coral tissue, lyophilized, and dissolved in DMSO. This organic whole tissue extract of *X. elongata* was initially tested for apoptosis induction. Apoptosis was assessed by an MTT assay on two isogenic mammalian epithelial cell lines, one apoptosis competent (W2) and the other apoptosis deficient (D3) (see below). The extract that induced apoptosis was subsequently purified by analytical RPHPLC. Using this strategy, nine pure compounds with proapoptotic activity were isolated from the whole tissue extracts. Chemical structures of the first four compounds were ascertained by standard spectroscopic techniques. The structures of compounds **1**–**4** were deduced as described below. Elucidation of the structures of the remaining five purified compounds is in progress.

The molecular formula of **1** was established as $C_{24}H_{34}O_6$ on the basis of HRESIMS [*m*/*z* 441.2250 $(M + Na)^+$ (calcd for $C_{24}H_{34}O_6Na$, 441.2253)]. This indicated a difference of an acetate group by comparison to the known compound xeniculin, isolated from *Xenia macrospiculata*.[8] The ^1H NMR of **1** indicated clearly the existence of the following functional groups: a 1-acetoxydihy-dropyran moiety [δ 5.87 (d, J = 1.3 Hz), H-1 and 6.55 (s), H-3], a terminal methylene [δ 4.78 (s) and 4.87 (s), H-19, H-19′], two methyls α to oxygen [δ 1.29 (s), H-16, H-17], an epoxy signal [δ 2.73 (t, J = 5.9 Hz), H-14], and a vinyl methyl group [δ 1.66 (s), H-18]. The NMR spectra of compound **1** and xeniculin were compared in $CDCl_3$ and were found to be similar, with the exception of the presence of a methylene group at C-9 [δ 25.1] instead of an oxygen-bearing carbon in xeniculin [δ 70.6], suggesting that **1** is 9-deacetoxyxeniculin.

The relative stereochemistry of **1** was established on the basis of ROESY data, coupling constant analyses, and chemical shift comparison to xeninculin,[8] tsitsixenicin A,[9,10] and related compounds.[10,8] The coupling constant (J = 12 Hz) between H-4a and H-11a suggests a trans ring junction. The small coupling constant (J = 1.3 Hz) between H-1 and H-11a would favor the α-position for H-1 if the six-membered ring was in a quasi-boat conformation. A closer look at the crystal structure of xenicin and essentially the six-membered ring (1-acetoxydihydropyran moiety), which is also present in **1**, suggests that H-1, if it is in the α-position, should display a ROESY cross-peak correlation to H-4a. In order to verify this suggestion, a high-scan ROESY experiment was performed. Careful analysis of the ROESY data, particularly in the cross-peak region of H-1 and H-4a, revealed unambiguously that these two protons display a ROESY correlation (Supporting Information). On the basis of this result, it appears that the configurations at C-1, C-4a, and C-11a in compound **1** are essentially the same as those in xeninculin, in which the protons H-1 and H-4a are on the α-face of the ring and the proton H-11a is oriented on the β-side. Previous attempts to establish the stereochemistry of an acetate group at C-12

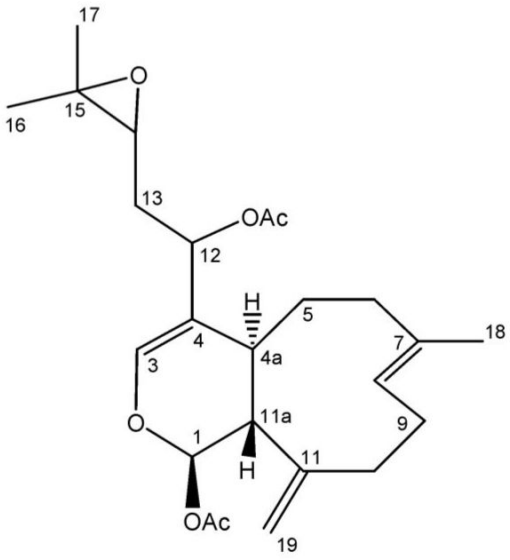

1

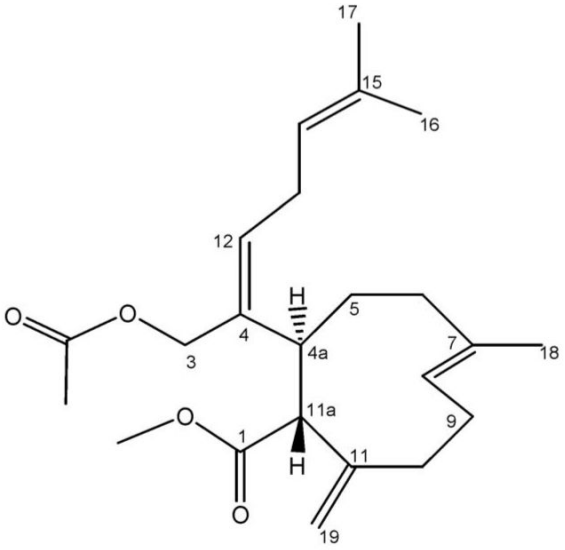

2

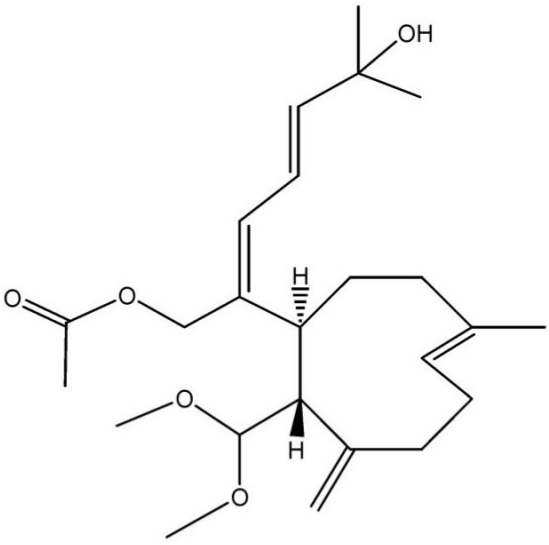

3

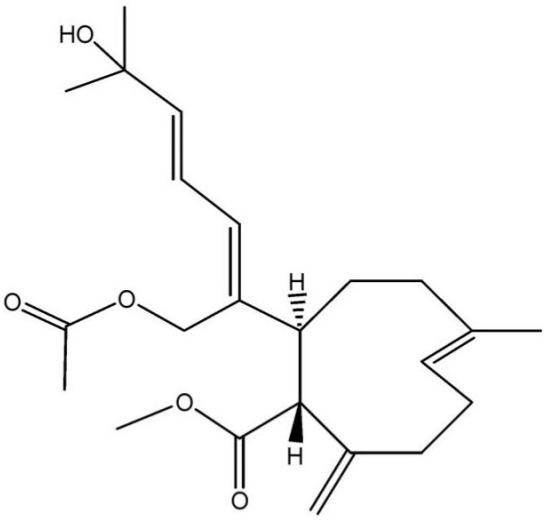

4

in xenicane diterpenes by chemical transformations and spectroscopy have failed,[10,11] and therefore the stereochemistry at C-12 remains unassigned. From the above results, the structure of **1** was formulated as shown.

A molecular formula of $C_{23}H_{34}O_4$ for **2** was determined from HRESIMS data. ^1H, ^{13}C NMR, DEPT, and multiplicity-edited HSQC of **2** indicated the presence of three olefinic methyls [δ 18, 18.3, 25.5, C-16, C-18, C-17], five methylenes [δ 28, 28.9, 32.5, 32.6, 39.9, C-13, C-9, C-5, C-10, C-6], two methines [δ 39.9, 61.7, C-4a, C-11a], one oxygen-bearing methylene [δ 66.5, C-3], one exocyclic methylene [δ 120.2, 144.2, C-19, C-11], three trisubstituted olefins [(δ 121.0, 133.5, C-14,C-15), (δ 139.5, 130, C-4,C-12), (δ 124.6,136, C-7,C-8)], two carbonyls [δ 172.7, 170.8, C-1, acetate moiety], one methyl belonging to the acetate group [δ 21.4]. and one methyl ester [δ 51.4]. All quaternary carbons [C-7, C-11, C-4, C-15] were positioned by

HMBC correlations: H-18 and C-7, H-10 and C-11, H-5 and C-4, and H-16, H-17 and C-15. On the basis of the COSY and HMBC correlations (Figure 1), **2** was considered to be a nine-membered monocarbocyclic ring belonging to the xenicane-type diterpenoid. Furthermore, the NMR spectroscopy of **2** was similar to those of umbellacin F,[12] except that the diol at C-14 and C-15 was missing in **2** and replaced by a double bond between C-14 and C-15; this suggests that umbellacin F[12] is the corresponding diol of **2**.

The relative stereostructure of **2** was investigated with the aid of a ROESY spectrum. The *E*-configuration was assigned to a $\Delta^{4(12)}$ double bond on the basis of the observed ROESY cross-peak between H-13b [δ 2.85] and H-4a [δ 3.30]. The *E*-configuration of the $\Delta^{7(8)}$ double bond was suggested by the observed ROESY cross-peak between H-18 [δ 1.55] and H-9a [δ 2.10]. The configuration of the two chiral centers at C-4a and C-11a was deduced by ROESY data and comparison with those of umballacin F.[12] The large coupling constant (J = 11 Hz) between H-4a [δ 3.30] and H-11a [δ 3.12] suggests that they have a configuration opposite of each other.[12,13] The observed ROESY cross-peak between H-3 [δ 4.53] and H-11a [δ 3.12] suggests that they have a similar configuration to umbellacin F.[12,14] Therefore the structure of **2** was established as shown.

The IR spectrum of **3** exhibited absorptions due to hydroxyl (3460 cm^{-1}) and carbonyl (1736 cm^{-1}) groups. HRESIMS and NMR data of **3** suggested a molecular formula of $C_{24}H_{38}O_5$. The NMR features of **3** closely resembled those of xenibecin[12,15] with the exception that an acetate group appears in **3** and one oxygenbearing methylene [δ 65.3, C-3] is also present in **3**. The strong HMBC correlations between the two methyl groups at δ 3.38 and 3.47 to the carbon at δ 105.0, C-1 suggest that these two methoxy groups are attached to the same carbon C-1, in contrast to that found in xenibecin,[12,15] in which one methoxy group is attached to carbon C-1 and the other methoxy group is attached to carbon C-3. The ^{1}H and COSY NMR spectra of **3** displayed an *E*-diene system at δ 6.00 (d, J = 11, H-12), 6.43 (dd, J = 11, 15, H-13), and 5.93 (d, J = 15, H-14). The olefinic methyl [δ 1.72 (s), H-18] and the exocyclic methylene [δ 4.65 (s), 4.80 (s), H-19, H-19′] were also present in **3**, as found in xenibecin.[12,15] One oxygen-bearing carbon [δ 70.8, C-15] was also present in **3** at the same position as that seen in xenibecin.[12,15] These above results indicate that the structure of **3** is similar to xenibecin, except that **3** is a nine-membered monocarbocyclic ring, whereas xenibecin is a trans-fused bicyclic ring.

The relative configuration of the two chiral centers at C-4a and C-11a was established by a ROESY experiment, coupling constant analyses, and comparison of chemical shifts to umbellacin G,[12] xenibecin,[15] and xenitacin.[15] The large coupling constant J = 11.5 Hz between H-4a and H-11a combined with the observed ROESY cross-peak between H-11a [δ 1.98] and H-3 [δ 4.53] indicated that the relative configurations of C-4a and C-11a are similar to those found in xenibecin. From these results the structure of **3** was formulated as shown.

The HRESIMS of **4** revealed that the molecular formula was $C_{23}H_{34}O_5$. The NMR data of **4** are closely similar to **3**, with the exception that only one signal of a methoxy group [δ 3.48] was present in the ^{1}H NMR of **4**. The ^{13}C NMR and HMBC data indicated two carbonyl signals: one belonged to the acetate group [δ 170.3] attached to C-3, and the other one was the carbonyl [δ 172.30, C-1] of the methyl ester moiety. The NMR data of **4** were also compared to those of xenibecin,[15] florlide F,[16] and 9-deoxyisoxeniolide-A,[17] which led to the conclusion that the structure of **4** is analogous to florlide F,[16] with the only difference in the ring system, in which one double bond appears between C-7 and C-8, similar to that found in the ring system of xenibecin and 9-deoxyisoxeniolide-A. The relative configuration at C-4a and C-11a was deduced by ROESY analysis. The observed ROESY cross-peak correlation between H-3, δ 4.53 and H-11a, δ 3.13, combined with the large coupling constant (J = 12 Hz) between H-4a and H-11a, suggested that these two protons, H-4a and H-11a, have trans configuration and

are comparable to H-4a (α-oriented) and H-11a (*β*-oriented) found in compound **3** as well as in xenibecin. The *E*-diene system was confirmed by the observed ROESY cross-peak correlation between H-12, H-14 and H-13, H-3 (Figure 2); therefore, the structure of **4** was established as shown. Thus, the four novel diterpenoid compounds possess similar structures never encountered before in marine natural products, essentially compounds **2**–**4**.

The use of methanol in the isolation procedure raises the question whether the methyl esters at C-1 in **2** and **4** and the two methyl ethers in **3** are "true" natural products or if they are adduct "artifacts" produced during the isolation process. To address this issue, the soft coral *X. elongata* was extracted with CH_2Cl_2. After fractionation by solid-phase extraction, followed by HPLC isolation, the chromatogram was compared to that of the fraction originally extracted by methanol (Supporting Information). The comparison revealed that the three compounds **2**–**4** were also present in the chromatogram from the fraction originally extracted by CH_2Cl_2. These three compounds were collected and analyzed by mass spectrometry and proton NMR. The results confirmed that compounds **2**–**4** are, indeed, natural products. Thus, the four novel diterpenoid compounds possess similar structures, which parallel their ability to induce apoptosis.

To develop a cell-based assay specific for the isolation and identification of apoptosis-inducing compounds that are potential anticancer agents, we took advantage of the recently defined mechanism of apoptotic signaling by members of the Bcl-2 family of apoptosis regulators. Two proapoptotic Bcl-2 family member proteins, Bax and Bak, are the functionally redundant, essential downstream regulators of apoptosis in the vast majority of apoptotic signaling pathways.[3-5] Moreover, Bax and Bak are essential for apoptotic function required for suppressing tumor growth and for mediating chemotherapeutic response.[18-23] These discoveries were made, in part, through the step-by-step engineering of immortal isogenic mouse epithelial cell lines derived from wild-type and mutant mice with targeted deletions in apoptosis regulators (*bax*, *bak*, *bim*, and others), separately and in combination.[6,20] Thus we have genetically matched immortal epithelial cell lines that have apoptosis function intact (wild-type W2) or disabled through specific genetic deletion of both *bax* and *bak* (D3) (U.S. Patent US 6,890,716). D3 cells, by virtue of being deficient in both Bax and Bak, are completely and irreversibly defective for apoptosis, yet all apoptosis regulatory mechanisms upstream (Bcl-2, Bim, etc.) remain intact. Importantly, the vast majority of human cancers with defects in apoptosis have the pathway disabled upstream of Bax and Bak. Thus, screening to identify compounds that have the capacity to kill W2 and not D3 cells should identify those that possess proapoptotic, and potentially anticancer, activity. Compounds that meet these criteria activate apoptosis upstream in a pathway that absolutely requires Bax and Bak. Moreover, compounds that indiscriminately kill both apoptosis-competent W2 and apoptosis-defective D3 cells are eliminated as nonspecifically toxic.

In order to assess the proapoptotic activities of these compounds as a marker for their potential anticancer efficacy, methanol-soluble fractions of *Xenia* extracts were tested for apoptosis induction in an MTT assay using the apoptosis-competent W2 and apoptosis-resistant D3 cells, as described above. Compounds **1**–**4** induce measurable cell death in W2 but not in D3 cells. To quantify apoptosis induction, viability was determined using an MTT assay.[24] Measurements were taken at time 0 and 48 h after addition of compounds in different concentrations. Viability was calculated as the difference between time 0 (addition of compound) and 48 h. Apoptosis induction was defined as at least 20% death of W2 cells and a 10% or higher growth of D3 cells by MTT assay. The optimal concentration of the compounds for apoptosis induction was determined on the basis of the dose–response of the two cells lines by MTT assay. The results (Figure 3A) reveal a significant induction of apoptosis by the whole tissue extract and by individual compounds, with the most remarkable induction shown by compound **1** (61% growth of D3 and 50% death of W2). Treatment of W2 and D3 cells with

0.1 μM staurosporine, a protein kinase inhibitor and potent inducer of apoptosis, was included as a positive control for apoptosis induction for comparison, which induced apoptosis at comparable levels to compound **1** (Figure 3A). Thus, the diterpenes we have isolated effectively and specifically activate apoptosis in immortalized mammalian epithelial cells.

In order to determine the differential impact of apoptosis induction on cell growth and viability of W2 and D3 cells, we monitored the cell division and viability by time-lapse microscopy. W2 and D3 cells were incubated for 48 h in the presence of compound **1** (12 μM) (Figure 3B). Both W2 and D3 cell lines showed comparable cell viability in the absence of the drug (Figure 3B). D3 cells retained their viability in presence of compound **1** even at 48 h, and this viability persisted following 72 h of treatment. There was, however, clear indication of growth arrest in the treated D3 cells. In stark contrast, W2 cells were highly sensitive to apoptosis induced by compound **1**. The apoptosis-competent W2 cells became rounded and detached from the surface between 18 and 24 h of treatment, displaying classic apoptotic morphology by time-lapse microscopy. Survival of the D3 cells for at least 72 h in contrast to the induction of cell death of W2 cells within 18–24 h of treatment with compound **1** suggests that compound **1** induced Bax- and Bak-mediated apoptosis. Taken together, these observations suggest that compound **1** induces apoptosis when the apoptosis pathway is intact and mediates cell growth arrest in the absence of a functional apoptosis pathway.

Soft corals belonging to the genus *Xenia* are a rich source of diterpenoids,[12,25] which are characterized by a nine-membered monocarbocyclic ring. The structures of *Xenia* diterpenoids have been divided into three groups: xenicins (containing a dihydropyran-cyclononane skeleton), xeniolides (possessing a δ-lactone-cyclononane skeleton), and xeniaphyllanes (with a bicyclo[7.2.0]undecane skeleton).[8,26] Xenicanes combine unique structural features with interesting biological activities; specifically, they often are cytotoxic against several murine and human cancer cell lines.[15,17]

A major limitation regarding the exploration of natural products from marine invertebrates, especially diterpenes, has been the difficulty in obtaining these compounds in sufficient quantities.[1,27] First, attempting to reisolate reasonable amounts of the same compound from the organism is difficult given the changing natural growth environment of these organisms. Second, the framework of nine-membered rings and the particular arrangement of functional groups with multiple embedded stereocenters limit the range of chemical reactions that are applicable to their synthesis. There is little in the existing synthetic literature to define an effective strategy for the synthesis of xenicanes.[27] The first total synthesis of an optically active xenicane diterpene has not yet been achieved.[27,28] However, we purified these compounds from *Xenia* grown under optimal conditions in a controlled environment that potentially facilitates reisolation of reasonable amounts of these compounds. In addition, an effort to synthesize these diterpenes is underway.

The compounds described here represent a potential platform for the identification of natural products with specific proapoptotic, and therefore anticancer, activities. This work describes bioactivity of four novel diterepenes from the soft coral *X. elongata* using a high-throughput cell-based screen that we have developed to identify compounds that induce apoptosis in precancerous mammalian epithelial cells. The vast majority of human solid tumors are of epithelial origin, and defects in apoptosis, mostly upstream of Bax and Bak, play important roles in both tumor suppression and mediation of chemotherapeutic response. Consequently, efforts are increasingly focused on developing drugs that can reactivate the apoptotic pathway. The compounds identified here induce apoptosis upstream of Bax and Bak and may have a potential for use as anticancer agents that exploit the apoptosis pathway in tumor cells.

Experimental Section

General Experimental Procedures

Optical rotations were measured on a JASCO P 1010 polarimeter. UV and FT-IR spectra were obtained employing Hewlett-Packard 8452A and Nicolet 510 instruments, respectively. All NMR spectra were recorded on Bruker Avance DRX300 and DPX400 spectrometers. Spectra were referenced to residual solvent signal with resonances at $\delta_{H/C}$ 7.26/77.1 ($CDCl_3$). ESIMS data were acquired on a Waters Micromass LCT Classic mass spectrometer and Varian 500-MS LC ion trap. HPLC separations were performed using Waters 510 HPLC pumps, a Waters 717 plus autosampler, and a Waters 996 photodiode array detector. All solvents were purchased as HPLC grade.

Extraction and Isolation Procedures

Live colonies of *Xenia elongata* were kept in optimal growing conditions (salinity 34 g/L, temperature 25 °C, light [min. 250 quanta m^{-2} s^{-1} and max. 500 quanta m^{-2} s^{-1}], pH 8.2–8.4) in the coral laboratory at the Marine Biotechnology Center, Institute of Marine and Coastal Sciences, Rutgers University. A voucher specimen is available as collection number SC/XE/Apr-04 System 1A. The soft coral was stored at −80 °C after addition of liquid nitrogen before workup. The material (80 g) was extracted three times, first with CH_2Cl_2 and then with MeOH, to give a nonpolar crude organic extract (259.2 mg) and a polar crude organic extract (537.9 mg). A portion of these two extracts (30 mg each) was tested for apoptosis induction. The polar crude organic extract was found active and subjected to fractionation by a solid-phase extraction cartridge (reversed-phase C18) to give three fractions using a stepwise gradient of H_2O–MeOH as solvent system. The fraction eluting with 15% H_2O and 85% MeOH had apoptosis induction activity. This fraction was further chromatographed on analytical RP HPLC (Phenomenex luna C8, 250 × 4.60 mm) using a gradient elution (starting with 80% H_2O and 20% CH_3CN, flow rate 1 mL/min) to yield successively 2.1 mg of **3** (t_R = 26 min), 4.3 mg of **1** (t_R = 29 min), 3 mg of **4** (t_R = 31 min), and 3 mg of **2** (t_R = 35 min).

Extraction of *X. elongata* with nonalcoholic solvent was performed with CH_2Cl_2. The material (40 g) was extracted four times with CH_2Cl_2 to give a crude organic extract (200 mg). This extract was fractionated by a solid-phase extraction cartridge (normal-phase) to give three fractions using a stepwise gradient of *n*-hexane–EtOAc as the solvent system. The fraction eluting with 50% n-hexane and 50% EtOAc was further chromatographed on analytical RP HPLC (Phenomenex luna C8, 250 × 4.60 mm) using a gradient elution (starting with 80% H_2O and 20% CH_3CN, flow rate 1 mL/min) to yield successively 1 mg of **3** (t_R = 26 min), 1.3 mg of **4** (t_R = 31 min), and 1.5 mg of **2** (t_R = 35 min).

Biological Evaluation: Apoptosis Induction

Apoptosis induction in the presence of compounds **1**–**4** was carried out in the following manner. W2 (apoptosis competent) and D3 (apoptosis defective) cells were plated in 96- and six-well plates and incubated for 24 h, after which they were evenly spread at about 50% confluency. At this time, compounds dissolved in DMSO and diluted in growth medium (DMEM) were added to the cells at various concentrations. DMSO concentration was kept at 0.5% in all wells. Plates were incubated for 24, 48, and 72 h. Cell viability was determined using a modification of the MTT assay,[24] where the reduction of yellow tetrazolium salt (MTT, 3-(4,5-dimethylthiazol-2-yl)-2,5) to purple formazan indicates mitochondrial activity, and thus cell viability. Cells were incubated with 0.5 mg/mL MTT for 3 h. Supernatant was aspirated, and DMSO was added to dissolve the formazan crystals. After 30 min incubation at 37 °C, with shaking, absorbance was read at 570 nm on a Spectra MAX 250 (Molecular Devices) plate reader. Differential growth from time 0 to 48 h was calculated. Starurosporine, an apoptosis inducer, and DMSO were used as positive and negative controls, respectively. Cells incubated

with compounds in six-well plates were visualized microscopically, and digital images were captured.

Computerized Video Time-Lapse Microscopy

Time-lapse microscopy was performed as previously described.[20] In summary, cells were cultured in the time-lapse chamber equipped with controlled environmental conditions. The time-lapse microscopy system consisted of an Olympus IX71 inverted microscope fitted with temperature-, humidity-, and CO_2-controlled environmental chamber (Solent Scientific, UK) and a Coolsnap ES cooled CCD camera. Image capturing and analysis were performed using Image-Pro Plus software (Media Cybernetics). Phase contrast images (100×) at multiple fields were obtained for the indicated time period. Time-lapse images were converted to movies using Image-Pro Plus software with custom modifications and a graphic data processing workstation (Dell Precision 670).

Compound 1—$[\alpha]^{22.5}_{D}$ −59 (*c* 0.87, $CHCl_3$); IR ν_{max} (neat) 3075, 2970, 2930, 2860, 1736, 1670, 1608, 1445, 1370, 1236, 1155, 1015, 950, 870, 835, 790 cm^{-1}; ^1H NMR and ^{13}C NMR, see Table 1; HRESIMS *m*/*z* 441.2250 (calcd for $C_{24}H_{34}O_6Na$, 441.2253).

Compound 2—$[\alpha]^{22.5}_{D}$ −21.2 (*c* 0.93, $CHCl_3$); IR ν_{max} (neat) 3075, 2970, 1736, 1380, 1370, 1155 cm^{-1}; ^1H NMR and ^{13}C NMR, see Table 2; HRESIMS *m*/*z* 397.2352 (calcd for $C_{23}H_{34}O_4Na$, 397.2354).

Compound 3—$[\alpha]^{22.5}_{D}$ +34 (*c* 0.3, $CHCl_3$); UV (MeOH) λ_{max} 225 nm (log ε 3.8); IR ν_{max} (neat) 3460, 1736, 1620, 1140 cm^{-1}; ^1H NMR and ^{13}C NMR, see Table 2; HRESIMS *m*/*z* 429.2618 (calcd for $C_{24}H_{38}O_5Na$, 429.2616).

Compound 4—$[\alpha]^{22.5}_{D}$ +40 (*c* 0.62, $CHCl_3$); UV (MeOH) λ_{max} 224 nm (log ε 3.8); IR ν_{max} (neat) 3460, 1736, 1620, 1140 cm^{-1}; ^1H NMR and ^{13}C NMR, see Table 2; HRESIMS *m*/*z* 413.2301 (calcd for $C_{23}H_{34}O_5Na$, 413.2303).

Supplementary Material

Refer to Web version on PubMed Central for supplementary material.

Acknowledgments

We thank K. McPhail for NMR data from NMR facilities at Oregon State University. We also thank A. Poulev for LC/MS analyses at Biotechnology Center for Agriculture and Environment, Rutgers University. We acknowledge F. Natale for culture of the organisms. This research was funded by Rutgers University through an Academic Excellence award and by the NIH (R37 CA53370 to E.W).

References and Notes

(1). Andrianasolo EH, France D, Cornell-Kennon S, Gerwick WH. J. Nat. Prod 2006;69:576–579. [PubMed: 16643029]

(2). Crews P, Gerwick W, Schmitz F, France D, Bair K, Wright A, Hallock Y. Pharm. Biol 2005;41 (Suppl. 1):39–52.

(3). Adams J. Genes Dev 2003;17:2418–2495.

(4). Danial N, Korsmeyer S. Cell 2004;116:205–219. [PubMed: 14744432]

(5). Gelinas C, White E. Genes Dev 2005;19:1263–1268. [PubMed: 15937216]

(6). Degenhardt K, White E. Clin. Cancer Res 2006;12:5274–5276. [PubMed: 17000659]

(7). Fesik SW. Nat. Rev. Cancer 2005;5:876–885. [PubMed: 16239906]

(8). Kashman Y, Groweiss A. J. Org. Chem 1980;45:3814–3824.

(9). Davies-Coleman MT, Beukes DR. S. Afr. J. Sci 2004;100:539–543.
(10). Hooper GJ, Davies-Coleman MT, Schleyer M. J. Nat. Prod 1997;60:889–893. [PubMed: 9322360]
(11). Coval SJ, Scheuer PJ, Matsumoto GK, Clardy J. Tetrahedron 1984;40:3823–3828.
(12). El-Gamal AAH, Wang S-K, Duh C-Y. J. Nat. Prod 2006;69:338–341. [PubMed: 16562830]
(13). Vanderah DJ, Steudler PA, Ciereszko LS, Schmitz FJ, Ekstrand JD, Van der Helm D. J. Am. Chem. Soc 1977;99:5780–5784. [PubMed: 18501]
(14). Miyamoto T, Takenaka Y, Yamada K, Higuchi R. J. Nat. Prod 1995;58:924–928. [PubMed: 7673938]
(15). Duh C-Y, El-Gamal AAH, Chiang CY, Chu C-J, Wang S-K, Dai C-F. J. Nat. Prod 2002;65:1882–1885. [PubMed: 12502332]
(16). Iwagawa T, Nakamura K, Hirose T, Okamura H, Nakatani M. J. Nat. Prod 2000;63:468–472. [PubMed: 10785415]
(17). El-Gamal AAH, Chiang C-Y, Huang S-H, Wang S-K, Duh C-Y. J. Nat. Prod 2005;68:1336–1340. [PubMed: 16180809]
(18). Degenhardt K, Sundararajan R, Chen G, Lindsten T, Thomson C, White E. J. Biol. Chem 2002;277:14127–14134. [PubMed: 11836241]
(19). Degenhardt K, Chen G, Lindsten T, White E. Cancer Cell 2002;2:193–203. [PubMed: 12242152]
(20). Degenhardt K, Mathew R, Beaudoin B, Bray K, Anderson D, Chen G, Mukherjee C, Shi Y, Gélinas C, Fan Y. Cancer Cell 2006;10:51–64. [PubMed: 16843265]
(21). Tan TT, Degenhardt K, Nelson DA, Beaudoin B, Nieves-Neira W, Bouillet P, Villunger A, Adams JM, White E. Cancer Cell 2005;7:227–238. [PubMed: 15766661]
(22). Nelson DA, White E. Genes Dev 2004;18:1223–1226. [PubMed: 15175258]
(23). White E. Cell Death Differ 2006;13:1371–1377. [PubMed: 16676007]
(24). Mosmann T. J. Immunol. Meth 1983;65:55–63.
(25). Anta C, Gonzalez N, Santafe G, Rodriguez JC. J. Nat. Prod 2002;65:766–768. [PubMed: 12027764]
(26). Cheng Y-B, Jang J-Y, Khalil AT, Kuo Y-H, Shen Y-C. J. Nat. Prod 2006;69:675–678. [PubMed: 16643051]
(27). Pollex A, Hiersemann M. Org. Lett 2005;7:5705–5708. [PubMed: 16321027]
(28). Mushti CS, Kim J-H, Corey EJ. J. Am. Chem. Soc 2006;128:14050–14052. [PubMed: 17061886]

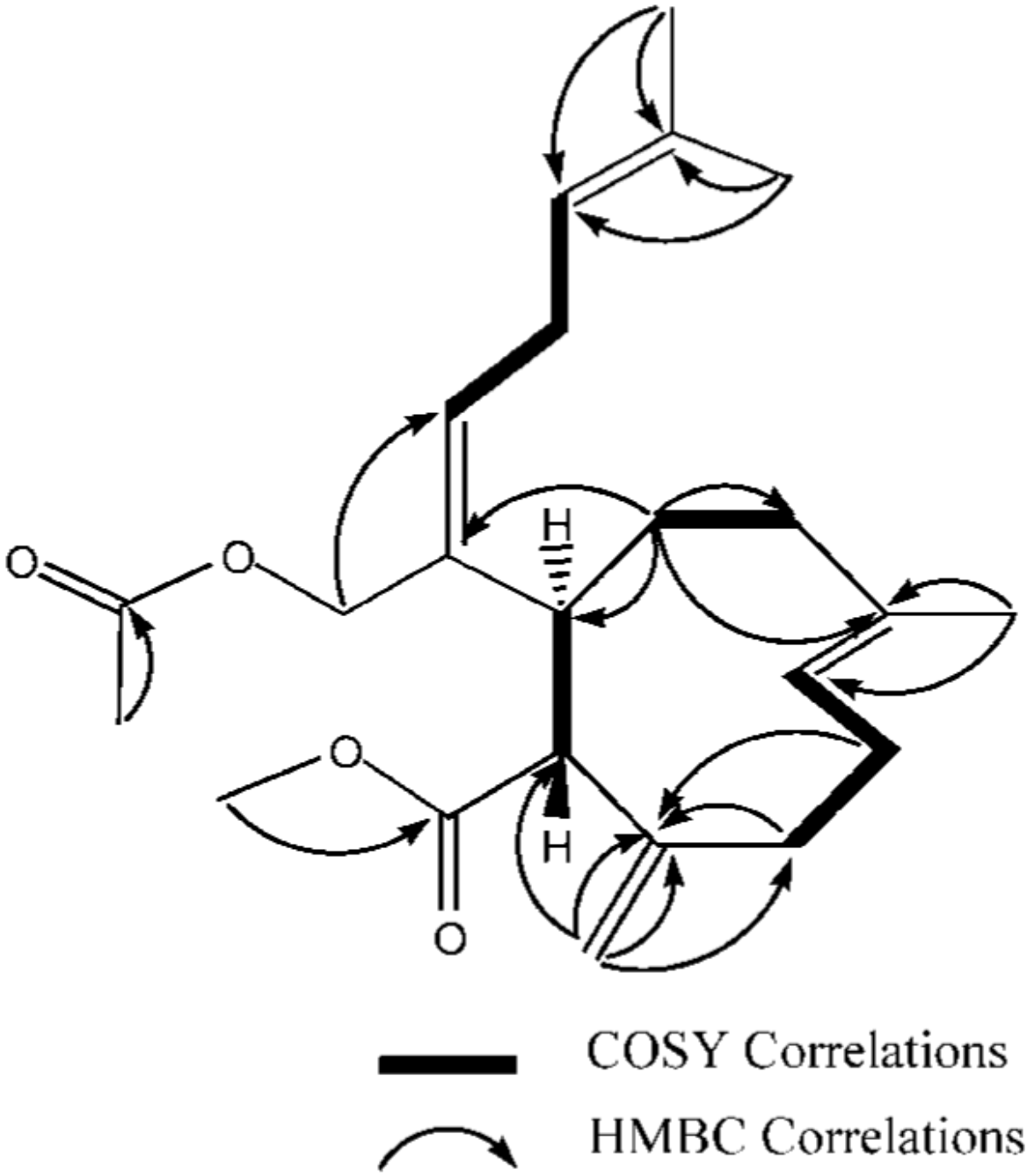

Figure 1.
Key HMBC and selected COSY correlations for compound **2**.

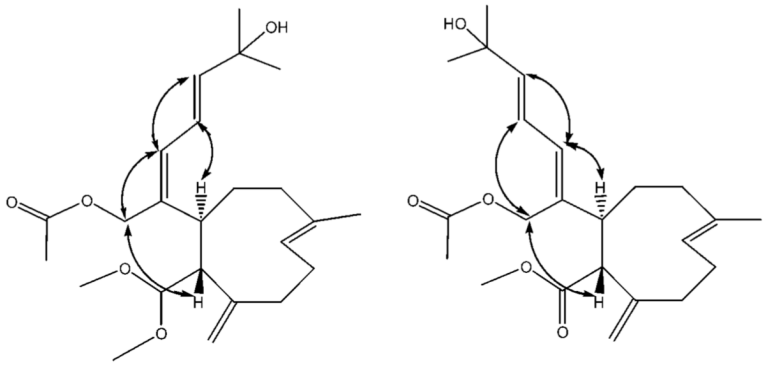

Figure 2.
Selected ROESY cross-peaks for compounds **3** and **4**.

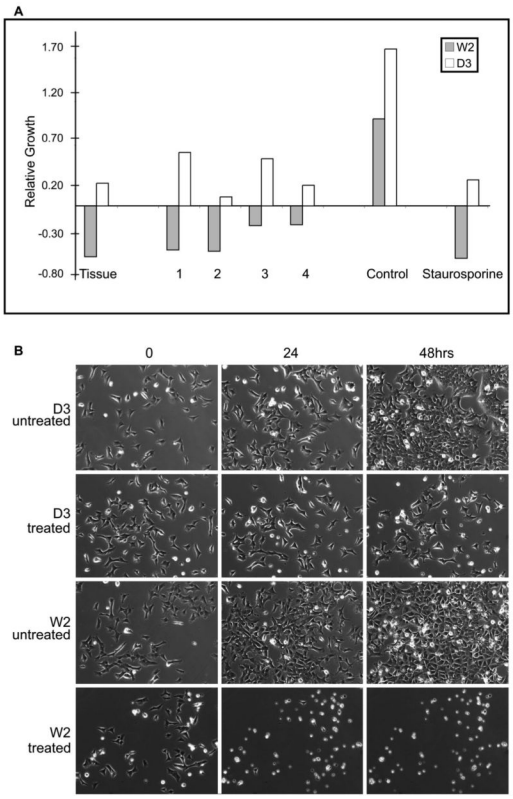

Figure 3.

(A) Change in relative W2 and D3 cell viability by MTT assay 48 h after addition of whole tissue extract, **1**, **2**, **3**, and **4** (**1** 12, **2** 29, **3** 12, **4** 11 μM). Staurosporine (0.1 μM), a known apoptosis inducer, and untreated cells were used as positive and negative controls. Values for the compounds are an average of five wells, with a standard deviation of less than 15% of the mean. (B) Compound **1** is a specific inducer of apoptosis in mammalian cells. The apoptosis-competent W2 cells and the apoptosis -resistant D3 cells were cultured in the presence or absence of compound **1** (12 μM) under normal physiological conditions (DMEM with 10% FBS, 5% CO_2 at 37 °C), and the cell viability was monitored by time-lapse microscopy. D3 cells were viable in the presence of compound **1** beyond 48 h, whereas the apoptosis-competent W2 cells showed massive apoptosis induction and significant loss of viability by 24 h of treatment.

Table 1

NMR Spectroscopic Data of Compound 1 (300 MHz, CDCl3)

position	δ_C	δ_H	HMBC[a]
1	91.7 CH	5.87, d (1.3)	3, 4a, CO
3	140.5 CH	6.55, s	1, 4, 4a, 12,
4	116.1 qC		
4a	36.7 CH	2.19, dd (8, 12)	3, 4, 5, 11
5	30.5 CH_2	1.50, m 1.90, m	4a, 6
6	40.2 CH_2	2.10, m 2.22, m	5, 7, 8
7	135.7 qC		
8	124.3 CH	5.40, t (5.9)	9
9	25.1 CH_2	2.50, m 2.10, m	8, 10
10	35.4 CH_2	2.27, m	11, 19
11	151.3 qC		
11a	49.9 CH	1.99, dd (1.3,12)	1, 4a, 11
12	72.4 CH	5.54, t (6.2)	3, 4, 4a, 13, 14, CO
13	32.7 CH_2	1.96, m	12, 14
14	60.9 CH	2.73, t (5.9)	13
15	58.0 qC		
16	19.0 CH_3	1.29, s	14, 15, 17
17	24.6 CH_3	1.29, s	14, 15, 16
18	17.7 CH_3	1.66, s	6, 7, 8
19	113.1 CH_2	4.78, s 4.87, s	10, 11, 11a,
CH_3 of CH_3COO	21.3 CH_3	2.06, s	CO
CO of CH_3COO	169.6 qC		
CH_3 of CH_3COO	21.3 CH_3	2.04, s	CO
CO of CH_3COO	170.4 qC		

[a]HMBC correlations, optimized for 8 Hz, are from proton(s) stated to the indicated carbon.

Table 2

^{1}H (300 MHz, $CDCl_3$) and ^{13}C (75 MHz, $CDCl_3$) NMR Data of Compounds **2**–**4**

	compound 2		compound 3		compound 4	
position	δ_C	δ_H	δ_C	δ_H	δ_C	δ_H
1	172.7 qC		105.0 CH	4.10, d (8.5)	172.3 qC	
3	66.5 CH_2	4.53, br s	66.0 CH_2	4.53, br s	66.5 CH_2	4.53, br s
4	139.5 qC		140.2 qC		140.1 qC	
4a	39.9 CH	3.30, m	44.2 CH	2.80, dd (7,12)	44.0 CH	2.72, m
5	32.5 CH_2	1.45, m 1.65, m	35.8 CH_2	2.33, m	35.9 CH_2	2.16, m
6	39.9 CH_2	2.10, m	39.9 CH_2	1.86, m 2.02, m	39.9 CH_2	1.90, m 2.01,m
7	136.0 qC		135.0 qC		135.5 qC	
8	124.6 CH	5.42, m	124.0 CH	5.43, m	124.5 CH	5.43, m
9	28.9 CH_2	2.10, m 2.40, m	28.7 CH_2	2.09, m 2.11, m	28.9 CH_2	2.10, m 2.38, m
10	32.6 CH_2	2.22, m 2.43, m	30.8 CH_2	2.16, m 2.20, m	32.6 CH_2	2.16, m 2.23, m
11	144.2 qC		144.0 qC		144.5 qC	
11a	61.7 CH	3.12, d (11.0)	56.1 CH	1.98, d (12)	61.8 CH	3.13, d (12.0)
12	130.0 CH	5.43, m	127.0 CH	6.00, d (11.0)	128.0 CH	6.02, d (11.0)
13	28.0 CH_2	2.80, m 2.85, m	120.0 CH	6.43, dd (11,15)	121.0 CH	6.40, dd (11,15)
14	121.0 CH	5.11, m	144.2 CH	5.93, d (15.0)	144.0 CH	5.70, d (15.0)
15	133.5 qC		70.8 qC		71.5 qC	
16	18.0 CH_3	1.64, d (1.1)	29.4 CH_3	1.35, s	29.5 CH_3	1.34, s
17	25.5 CH_3	1.72, d (1.1)	29.4 CH_3	1.35, s	29.5 CH_3	1.35, s
18	18.3 CH_3	1.55, s	18.2 CH_3	1.72, s	19.0 CH_3	1.60, s
19	120.2 CH_2	5.04, s 5.10, s	111.0 CH_2	4.65, s 4.80, s	120.1 CH_2	5.04, s 5.10, s
CH_3 of CH_3COO	21.4 CH_3	2.06, s	21.2 CH_3	2.07, s	21.2 CH_3	2.04, s
CO of CH_3COO	170.8 qC		170.9 qC		170.4 qC	
CH_3 of CH_3OCO	51.4 CH_3	3.56, s			51.2 CH_3	3.48, s
CO of CH_3OCO	172.7 qC				172.3 qC	
CH_3O			56.0 CH_3	3.38, s		
CH_3O			55.0 CH_3	3.47, s		